Insights into the Southern Oklahoma Aulacogen Using

Gravity Model Comparisons of the Reelfoot Rift

BY

KERRI MELISA GEFEKE
B.A., Augustana University, 1999
B.S., Northern Illinois University, 2017

THESIS

Submitted as part fulfillment of the requirements
for the degree of Master of Science in Earth and Environmental Sciences
in the Graduate College of the
University of Illinois at Chicago, 2019

Chicago, Illinois

Defense Committee:

Carol Stein, Chair and Advisor
Andrew Dombard
Stefany Sit

This thesis is dedicated to my wife, Kristin Bush. Your love and support are everything.

ACKNOWLEDGEMENTS

I would like to thank my advisor, Dr. Carol Stein for her firm and steady guidance and support during my graduate studies and provided the inspiration for this study. Additionally, my thesis committee, Carol Stein, Andrew Dombard, and Stefany Sit provided timely feedback and critical insight throughout the process. I would also like to acknowledge Lee Falkena for his assistance and leadership as I developed in my role as teaching assistant. Finally, I would like to thank Mr. Dave Berner, my first geology professor. Your class gave me the inspiration to change the course of my life.

KMG

TABLE OF CONTENTS

LIST OF TABLES

LIST OF FIGURES

LIST OF FIGURES (continued)

LIST OF ABBREVIATIONS

RMSE	Root Mean Square Error
RR	Reelfoot Rift
SOA	Southern Oklahoma Aulacogen

SUMMARY

A comparative study of the Reelfoot Rift and Southern Oklahoma Aulacogen was completed using gravity modeling. The study's aim was to answer four questions: What effect do geologic structures such as rift pillows, sedimentary basins, and rift inversions have on gravity values? Do the gravity data of the Southern Oklahoma Aulacogen support the existence of a rift pillow? Can the Reelfoot Rift and Southern Oklahoma Aulacogen be considered analogs of one another at different stages of rift evolution? Why are the gravity profiles for these rifts so different? Multiple models were made to resolve these questions.

Twenty schematic models were created to investigate the effect of rift pillows, sedimentary basins, and rift inversion on gravity anomalies. Models of the Southern Oklahoma Aulacogen were built to determine if its gravity data support the existence of a rift pillow. Finally, models were created to compare the conditions of the Reelfoot Rift and Southern Oklahoma Aulacogen directly. The fit of the models was considered utilizing root-mean-square error analysis.

The schematic models showed that rift pillows produce positive gravity anomalies, sedimentary basins produce negative gravity anomalies, and rift inversions bring the pillows closer to the surface increasing the strength of the gravity anomaly. The Southern Oklahoma Aulacogen models demonstrated that its observed gravity anomaly could be consistent with a 5 to 10 km thick rift pillow. Comparison of models between the Southern Oklahoma Aulacogen and Reelfoot Rift required inversions or "subsidence" (uninversions). In this study, the Southern Oklahoma Aulacogen (which is currently

inverted or uplifted by 12 km) was ‘subsided’ by 10.5 km and compared to the observed Reelfoot Rift (which is inverted by 1.5 km). Additionally, the Reelfoot Rift was inverted by 10.5 km and compared to the Southern Oklahoma Aulacogen. Ultimately, these rifts demonstrated a similarity that is masked by pre-rift geology and post-rift crustal modifications.

1. INTRODUCTION

1.1 Continental Rifts

1.1.1 Defined

Paleorifts, failed rifts with no present-day thermal anomaly or geophysical evidence of active extension, are our best record of processes and structures from the early stages of continental breakup (Baldridge et al., 1995). A continental rift is an elongate tectonic depression approximately 20-100 km wide associated with modification of the lithosphere by extension (Brun and Choukroune, 1983; Olsen and Morgan, 1995). A broader definition of rifts also includes any zone of splitting or extension where the breakup of continental lithosphere has not or did not proceed to seafloor spreading, including both the narrow Red Sea and the wide Basin and Range Province (Buck, 2007). In contrast, successful continental rifting forms conjugate passive margins a few 100 km wide between undeformed continental crust and oceanic crust separated by seafloor spreading (Brun and Choukroune, 1983).

1.1.2 Evolution of Continental Rifts

While the development of individual rifts depends on their specific tectonics, rifts develop along a common evolutionary sequence (Figure 1; Burke and Dewey, 1973; Olsen and Morgan, 1995; Stein et al., 2018). The beginning stages of rifting are similar to the presently opening Baikal or Kenya Rifts (Figure 1A). Rifts have three possible end stages: 1) an oceanic basin with seafloor spreading and relict rift features at the two passive margins; 2) a failed non-inverted intracontinental rift; or 3) a failed inverted intracontinental rift. An inverted rift is one in which subsequent regional compression causes shortening, resulting in uplift along originally normal faults and newer-formed reverse faults (Williams et al., 1989). Because rifts are zones of crustal weakness, they may have multiple cycles of reactivation over time (Howe, 1985; Kolata and Nelson, 1991). For example, multiple inversion episodes resulted in 7 km of inversion (uplift) on the Keweenaw fault within the Midcontinent Rift (Stein et al., 2015; Figure 1D). The amount of inversion may be affected by factors including: the time since rifting; crustal and

lithospheric thickness, composition, and rheology; and thermal structure including amount of crustal and mantle thinning and/or melting (Huismans and Beaumont, 2009).

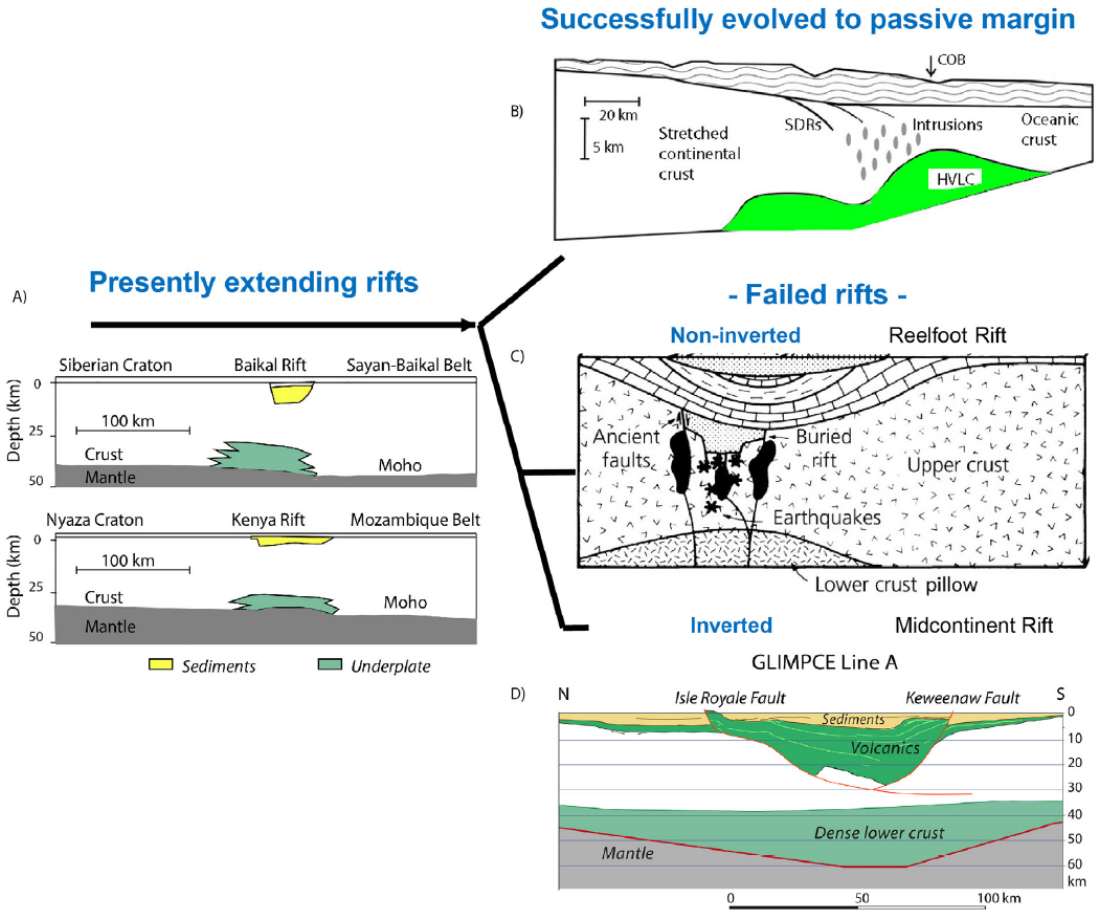

Figure 1. Suggested rift evolutionary sequence from Stein et al. (2018). Frames are from A) Thybo and Artemieva (2013), B) Schnabel et al. (2008), C) Braile et al. (1986), and D) Stein et al. (2015) modified from Green et al. (1989). In frame B) COB signifies continent-ocean boundary, SDR signifies seaward dipping reflectors, and HVLC signifies high-velocity lower crustal bodies. Note that each frame has a high-density lower crust, underplate, or lower crust pillow indicated above the mantle.

The Southern Oklahoma Aulacogen, an inverted, failed rift with 12 km of uplift, is analogous to the Midcontinent Rift (Figure 1D; Ham and Wilson, 1967; Perry, 1989; Robbins and Keller, 1992). In

contrast, the Reelfoot Rift (Figure 1C) is a mostly non-inverted, failed rift that preserves a mostly undisturbed post-rift subsidence stage (Stein et al., 2018). Fossil rift margins undergo subsidence from thinning of the continental crust, thermal subsidence, and sediment loading, leading to them often being overlaid by intracratonic basins (Ingersoll, 2012). The Southern Oklahoma Aulacogen abuts the Anadarko Basin, which contains approximately 12 km of mid-to-late Cambrian through Permian sediments (Ham and Wilson, 1967; Perry, 1989). The Reelfoot Rift is overlaid by the southern end of the Illinois Basin and contains approximately 7 km of Cambrian to Pennsylvanian sedimentary rocks (Kolata and Nelson, 1991; Dart and Swolfs, 1998).

Rift zones often have an underplated, high-density lower crust layer (Mooney et al., 1983; White and McKenzie, 1989). Also called rift pillows, these layers are likely due to the residuum from mafic magma upwelling from the mantle during rifting (Zoback and Richardson, 1996; Thybo and Artemieva, 2013). The Reelfoot Rift has a high-density mafic layer (Stuart et al., 1997), but one has not been identified below the Southern Oklahoma Aulacogen.

1.1.3 **The Southern Oklahoma Aulacogen and Reelfoot Rift**

The Reelfoot Rift and the Southern Oklahoma Aulacogen formed in the same continental rifting event (Section 2), but few studies have compared these fossil rifts. Early studies noted similarities between the basin associated with the Reelfoot Rift and other intracontinental rift basins such as the Anadarko Basin (Southern Oklahoma Aulacogen) and the Lake Superior Basin (Midcontinent Rift) (Braile et al., 1986). Each rift was evaluated relative to the Midcontinent Rift (Stein et al., 2018), and the Southern Oklahoma Aulacogen was compared to the Dniepr-Donets Aulacogen in the Baltic region (Keller and Stephenson, 2007). One observation from these studies is the difference between the gravity signatures of the Reelfoot Rift and Southern Oklahoma Aulacogen. The Reelfoot Rift has a Bouguer gravity low, whereas the Southern Oklahoma Aulacogen has a Bouguer gravity high (Section 2).

1.1.4. **Purpose of the study**

The purpose of this study is to compare the Reelfoot Rift and Southern Oklahoma Aulacogen based on geologic history, subsurface structure, and gravity data. Ultimately, this study was designed to answer four questions:

1) What effect do geologic structures such as rift pillows, sedimentary basins, and rift inversions have on gravity values?
2) Does the gravity data of the Southern Oklahoma Aulacogen support the existence of a rift pillow?
3) Can the Reelfoot Rift and Southern Oklahoma Aulacogen be considered analogs of one another at different stages of rift evolution?
4) Why are the gravity profiles for these rifts so different?

The effect of geologic structures on gravity profiles is explored in Section 4.1 through the calculation of gravity anomalies for simple schematic models with rift pillows and sedimentary basins for inverted and non-inverted rifts. Whether the gravity data of the Southern Oklahoma Aulacogen can support the existence of a rift pillow is explored in Section 4.3 by modeling possible rift pillows below the Southern Oklahoma Aulacogen of various thickness and densities. Finally, whether the Reelfoot Rift and Southern Oklahoma Aulacogen can be considered analogs of one another at different evolutionary stages and why their current gravity profiles are so different is considered in Sections 5.1 and 5.2. The results of this study are a more thorough understanding of the gravity effects of rift dynamics through the comparison of these paleorifts, building upon recent other rift comparison studies (Mooney et al., 1983; Braile et al., 1986; Keller and Stephenson, 2007; Stein et al., 2018) and the identification of additional avenues for future research.

2. REVIEW OF THE REELFOOT RIFT AND SOUTHERN OKLAHOMA AULACOGEN

2.1 Geological Background

The Reelfoot Rift and Southern Oklahoma Aulacogen are in the central interior of the North American continent (Figure 2). These rifts formed during the Late Precambrian (about 560-550 Ma) breakup of Pannotia (a short-lived supercontinent that existed from about 650-560 Ma) and the opening of the Iapetus Ocean between Gondwana and Laurentia with the detachment of the Argentine Precordillera from the Ouachita embayment (Dalziel, 1997; Whitmeyer and Karlstrom, 2007; Scotese, 2009). These paleorifts are aulacogens, the failed third arm of triple junctions (Burke and Dewey, 1973; Ervin and McGinnis, 1975; Burke, 1977; Perry, 1989; Thomas, 1991; Olsen and Morgan, 1995; Brueseke et al., 2016). Later, during the late Paleozoic and Mesozoic (335-175 Ma), collisions of North America with South America and Africa during the formation of supercontinent Pangaea caused the Southern Oklahoma Aulacogen to undergo up to 12 km of inversion (Ham and Wilson, 1967; Perry, 1989; Robbins and Keller, 1992), whereas the Reelfoot Rift only underwent slight (up to 1500 m) inversion (Dart and Swolfs, 1998; Csontos et al., 2008). Both regions experienced seismicity in the Quaternary period. The Southern Oklahoma Aulacogen has been relatively stable except for isolated Holocene movement along the Meers fault, most recently in two left-lateral events in about 1300 BP and 2500 BP (Swan et al., 1993). The Reelfoot Rift, however, is located within the broader New Madrid Seismic Zone, which has been associated with seismicity into modern times, including the large earthquakes of 1811-1812 (Braile et al., 1986).

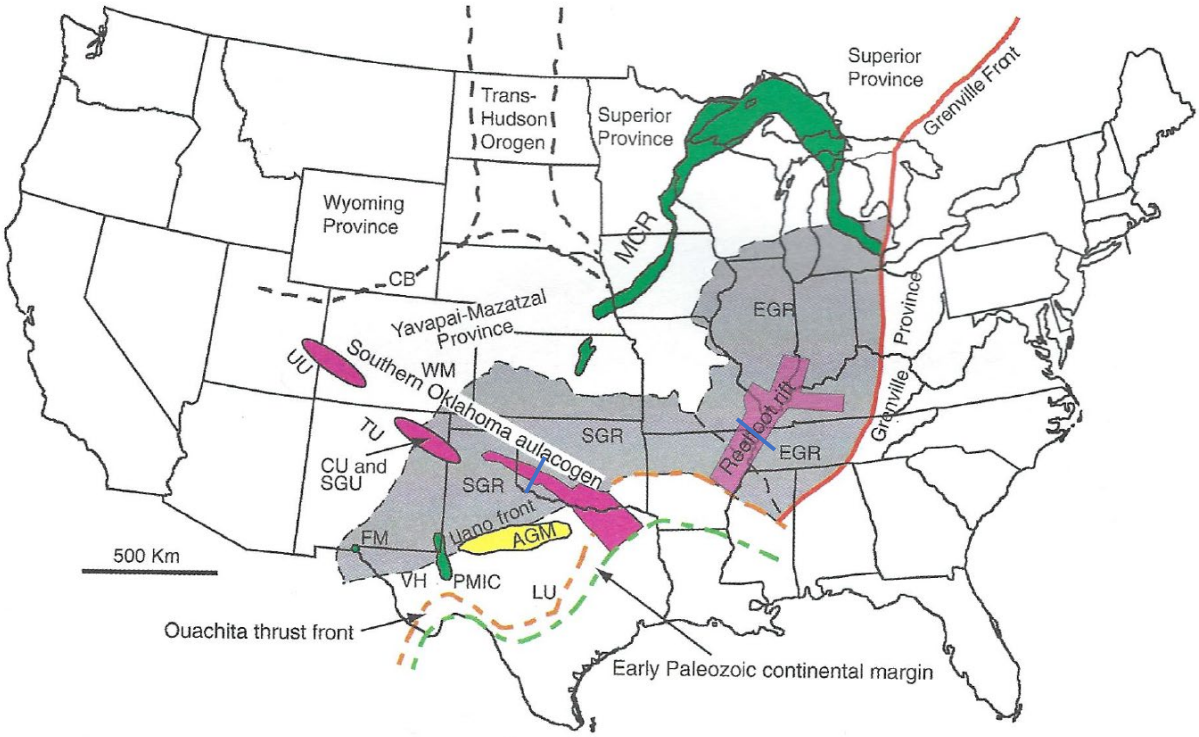

Figure 2. North American continent with paleorifts. MCR = Midcontinent Rift; UU = Uncompahgre uplift; TU = Tusas uplift; CU = Cimarron uplift; SGU = Sierra Grande uplift; SGR = southern granite-rhyolite province; EGR eastern granite-rhyolite province; FM = Franklin Mountains; VH = Van Horn area; PMIC = Pecos mafic intrusive complex; LU = Llano uplift; AGM = Abilene gravity minimum; CB = Cheyenne belt; WM = Wet Mountains (Keller and Stephenson, 2007). Blue line indicates approximate locations of cross-sections for the Reelfoot Rift in Figure 4 and the Southern Oklahoma Aulacogen in Figure 6.

2.2 **Reelfoot Rift**

The Reelfoot Rift extends from the far northern end of the Mississippi Embayment in east-central Arkansas along the border of Missouri, Tennessee, and Kentucky into the southern end of the Illinois Basin (Figures 2 and 3). The Reelfoot Rift is a failed rift with a 300-km-long northeast-trending graben and a 70-km-wide depression based on regional geology (Burke and Dewey, 1973; Dart and Swolfs, 1998). Geophysical data including gravity, aeromagnetic, and seismology surveys give insight into its structure (Ervin and McGinnis, 1975; Kane et al., 1981; Mooney et al., 1983; Nelson and Zhang, 1991; Dart and Swolfs, 1998; Catchings, 1999; Chen et al., 2014; Pollitz and Mooney, 2014; McGlannan and

Gilbert, 2016). Synrift and postrift deposition and subsidence created a broad basin that filled with up to 7 km of sediments (Howe and Thompson, 1984; Kolata and Nelson, 1991; Dart and Swolfs, 1998). Collisions forming Pangaea in the late Paleozoic likely reactivated the Reelfoot Rift resulting in perhaps 1500 m of compressional inversion (Dart and Swolfs, 1998; Csontos et al., 2008).

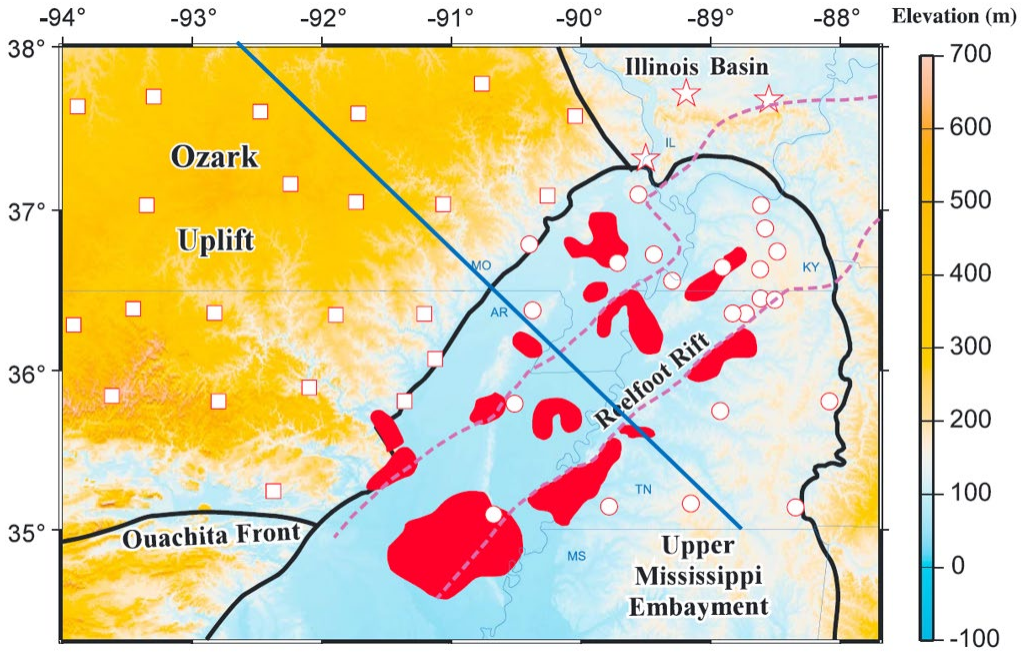

Figure 3. Regional map of the Reelfoot Rift and profile from Liu et al. (2017). The area between the purple dashed line is the Reelfoot Rift. Blue line marks location of cross-section in Figure 4. Red areas are igneous bodies. Circles, squares, and stars are seismic station locations.

For this study, I use Liu et al.'s (2017) model for the Reelfoot Rift (Figure 4). The authors constrained their subsurface structure model with their study's crustal thickness and velocity results along with gravity and magnetic data (Hildenbrand, 1985) and seismic refraction data (Mooney et al., 1983) (Liu et al., 2017).

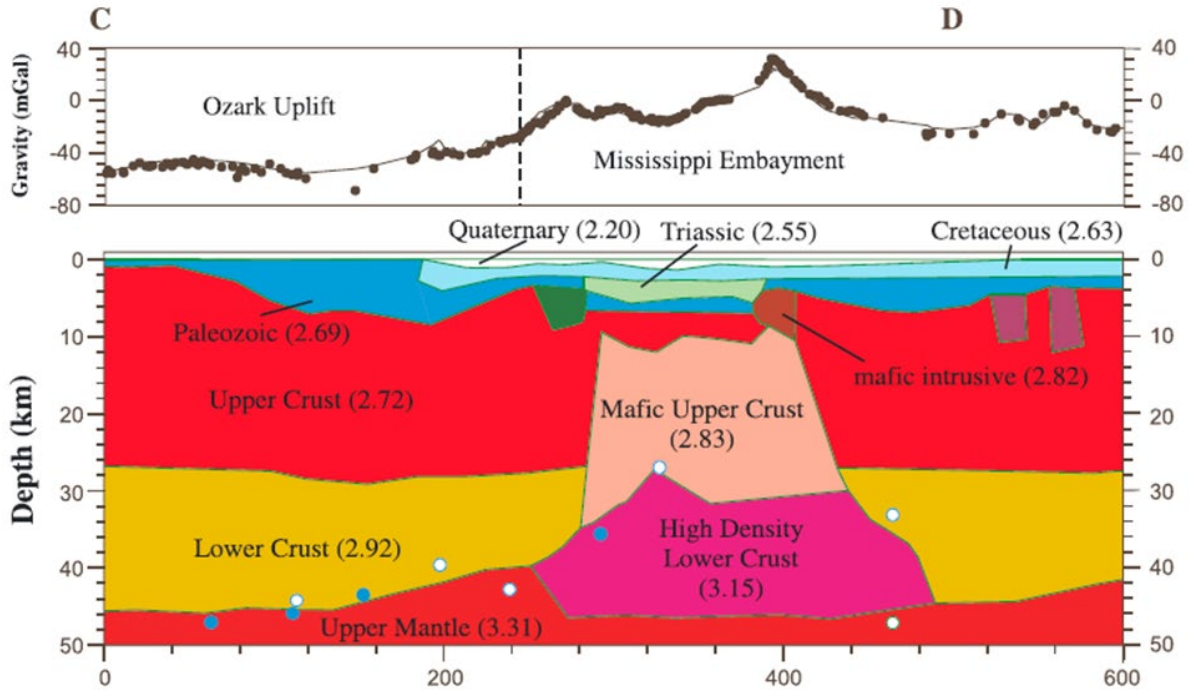

Figure 4. Bouguer gravity profile and modeled subsurface structure across the Reelfoot Rift (Liu et al., 2017). Green and purple bodies below Paleozoic layer are additional mafic intrusive bodies. Blue and white circles represent seismic data collected from Transportable Array stations. Pink layer labeled as High Density Lower Crust is the rift pillow.

2.3 **Southern Oklahoma Aulacogen**

The Southern Oklahoma Aulacogen (SOA), situated along the southern edge of the Anadarko Basin, trends WNW-ESE parallel to the Wichita Uplift (Figure 5). It shows good spatial correlation between magnetic highs and gravitational anomalies (Keller and Baldridge, 1995; Erkan, 2015). Post-rift sedimentation with major subsidence throughout the Paleozoic (Perry, 1989) resulted in the rifts abutting and/or being partially overlain by the up to 12-km-deep Anadarko Basin. Pennsylvanian-age deformation from tectonic collision with Gondwana during the formation of Pangaea (Perry, 1989) led to the Wichita uplift and vertical displacements up to 12 km (Ham and Wilson, 1967; Perry, 1989; Robbins and Keller, 1992). USArray Transportable Array data have been used to constrain the structure

of the crust and upper mantle in the region (Evanzia et al., 2014; Gallegos et al., 2014; Pollitz and Mooney, 2016; Ekström, 2017).

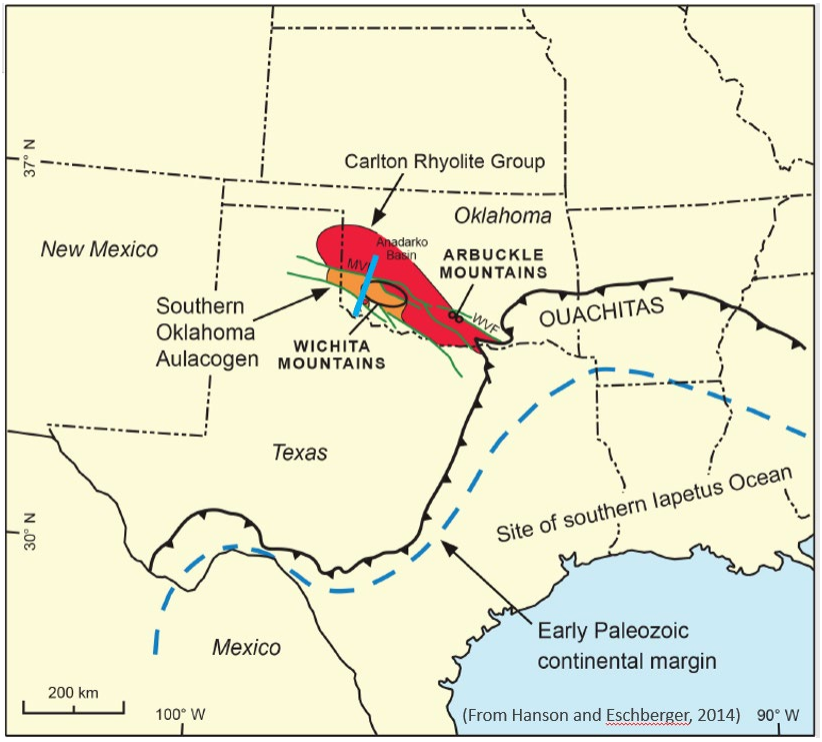

Figure 5. Southern Oklahoma Aulacogen on North America Paleozoic continental margin adapted from Hanson and Eschberger (2014). Red and orange outlined areas show extent of Wichita Igneous Province in the subsurface. Green lines are faults: MVF: Mountain View Fault; WVF: Washita Valley Fault. Blue line is location of Southern Oklahoma Aulacogen cross-section in Figure 6.

As a starting point for my study, I use Keller and Stephenson's (2007) model (Figure 6), which is constrained by gravity and seismic data (Brewer et al., 1983; Chang et al., 1989; Robbins and Keller, 1992; Keller and Stephenson, 2007).

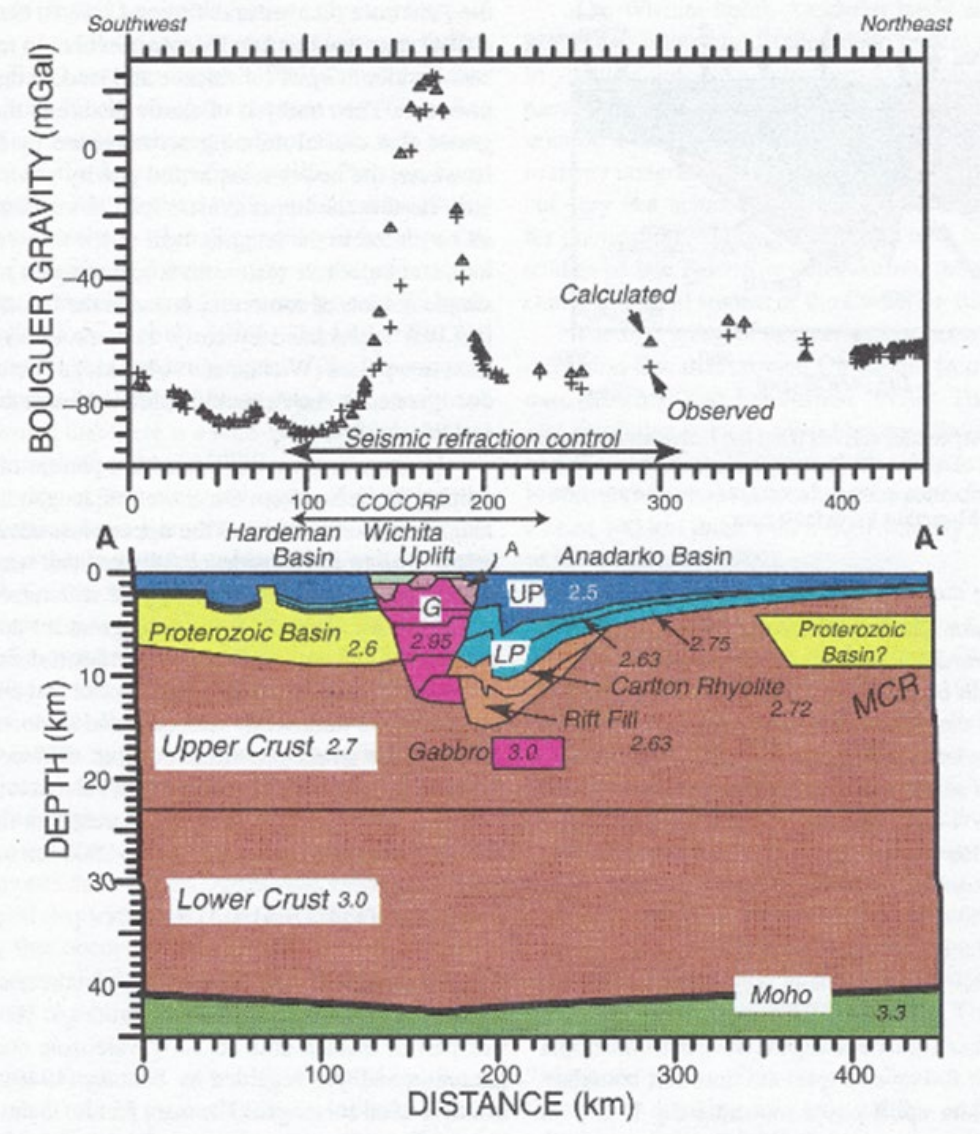

Figure 6. Gravity profile and modeled subsurface structure across the Southern Oklahoma Aulacogen (Keller and Stephenson, 2007). A: felsic intrusions and volcanics (2.7 g/cm^3); G: gabbroic intrusions (2.75, 2.8, 2.95, 3.05, and 3.10 g/ cm^3 from top to bottom); UP: upper Paleozoic strata; LP: lower Paleozoic strata; MCR: Midcontinent Rift. Light green layer is younger than Paleozoic strata.

3. GRAVITY PROFILE ANALYSIS

3.1 Gravity anomalies

The value of gravity at Earth's surface depends on surface elevation, latitude, and density variations with depth. Gravity anomalies are the measured gravity minus the expected value. My study uses Bouguer gravity anomalies, the observed gravity minus correction for latitude, elevation, height above sea-level, and attraction of terrain, to assess differences in subsurface rock densities.

Analysis of the gravity profile involves matching observations with subsurface models. The commonly used indirect, or iterative, method (Lowrie, 2004) involves fitting a model of the subsurface to the gravity profile through trial and error (Bott and Hinze, 1995). Because there are innumerable ways to model the subsurface, the model is constrained with other geological and geophysical data to narrow the interpretation.

3.2 Gravity data modeling

I used a forward gravity modeling program (Salayandia et al., 2004) that uses the polygonal method (Talwani et al., 1959; Cady, 1980). The user inputs the X, Y coordinates of each point of the polygon along with density and the observed gravity profile. The result can be manipulated using a graphical user interface. Manipulating the densities or locations of the subsurface bodies will change the calculated gravity profile. The model's calculated gravity profile is compared with the observed profile with a Root Mean Square Error (RMSE) analysis to assess the validity of the model.

To test my ability to use the modeling program, I compared my results to Southern Oklahoma Aulacogen and Reelfoot Rift profiles (Keller and Stephenson, 2007; Liu et al., 2017). I recreated the data used in these studies and their subsurface models using WebPlotDigitizer Version 3.9 (Rohatgi, 2015) to recover the numerical values of the data in an X, Y format. These data were input into Excel for

processing and/or retrieval before inputting them into the Talwani program. I then reproduced the published results with this program.

4. RESULTS

4.1 Schematic Models

To understand how gravity for a failed non-inverted rift compares to that for an inverted one, I calculated gravity anomalies for models with rift pillows and sedimentary basins of varying thickness (and varying amounts of inversion). These structures are important because they are the primary differences between the Reelfoot Rift (a mostly non-inverted, thick sedimentary basin with a rift pillow) (Figure 4; Stuart et al., 1997) and the Southern Oklahoma Aulacogen (a severely inverted rift, but no identified rift pillow) (Figure 6).

I created 20 simplified models to test the effects of rift pillows, sedimentary basins, and rift inversions (Table I). The models assume that uplift of the rift from inversion is eroded, so the maximum elevation is constant in all models. These models include rift pillows of 5, 10, and 15 km thicknesses that have been inverted by 5, 10, and 15 km. Other models have sedimentary basins 5, 10 and 15 km thick and inversions of 5 or 10 km. The models include a crust with a density of 2700 kg/m^3, a rift pillow with a density of 2900 kg/m^3, a sedimentary basin with a density of 2500 kg/m^3, and a mantle layer at 40 km depth with a density of 3300 kg/m^3 compared to a Bouguer gravity baseline of 0 mGal.

The thickness and depth of the rift pillow controls the size of the positive gravity anomaly. For example, model 1 has a 5 km thick rift pillow and a maximum gravity anomaly of 11 mGal, whereas model 9 has a 15 km thick rift pillow and a maximum gravity anomaly of 65 mGal (Figure 7). Inversions of rifts uplift the crust and bring the denser rift pillows nearer to the surface, increasing the gravity anomaly. For example, model 11 has a 15 km thick rift pillow with a tectonic inversion of 10 km, yielding a maximum gravity of 178 mGal (Figure 7).

Model #	Model Description	Gravity Results (mGal)	Model #	Model Description	Gravity Results (mGal)	Model #	Model Description	Gravity Results (mGal)	Model #	Model Description	Gravity Results (mGal)
1	Rift Pillow - 5km	11	**6**	Rift Pillow - 10km with 5km inversion	80	**11**	Rift Pillow - 15km with 10km inversion	198	**16**	Sedimentary Basin - 10km with 5km inversion	-28
2	Rift Pillow - 5km with 5km inversion	54	**7**	Rift Pillow - 10km with 10km inversion	147	**12**	Rift Pillow - 15km with 15km inversion	253	**17**	Sedimentary Basin - 10km with 10km inversion	-23
3	Rift Pillow - 5km with 10km inversion	118	**8**	Rift Pillow - 10km with 15km inversion	220	**13**	Sedimentary Basin - 5km	-36	**18**	Sedimentary Basin - 15km	-94
4	Rift Pillow - 5km with 15km inversion	189	**9**	Rift Pillow - 15km	66	**14**	Sedimentary Basin - 5km with 5km inversion	-18	**19**	Sedimentary Basin - 15km with 5km inversion	-60
5	Rift Pillow - 10km	36	**10**	Rift Pillow - 15km with 5km inversion	109	**15**	Sedimentary Basin - 10km	-65	**20**	Sedimentary Basin - 15km with 10km inversion	-22

Table I. Summary of schematic models. Gravity results are the maximum value (either positive or negative) produced by the model.

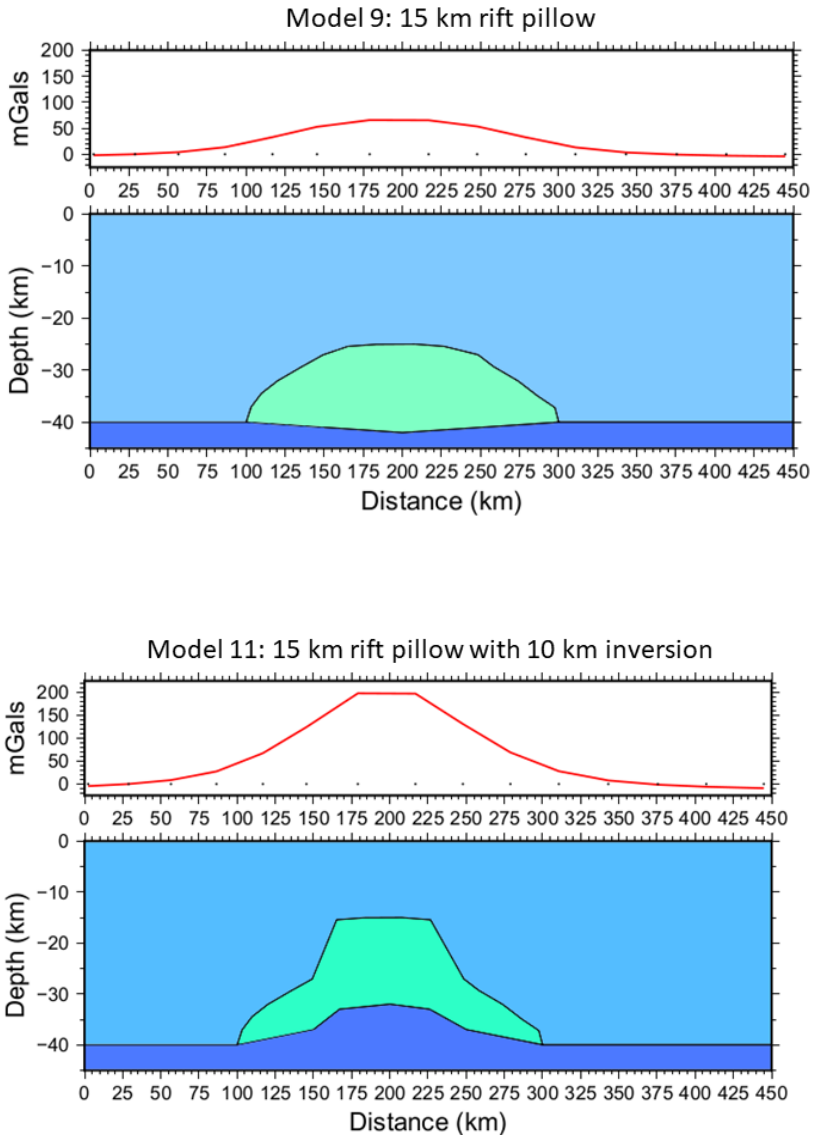

Figure 7. Schematic gravity models 9 (top) and 11 (bottom). Black dots are gravity at 0 mGal, red line is calculated gravity, light blue layer is crust, light green layer is rift pillow, and dark blue layer is mantle. Model 9 (top) illustrates a 66 mGal gravity anomaly created by a 15 km rift pillow, and model 11 (bottom) demonstrates a 3-fold increase in the gravity anomaly to 198 mGal when the rift pillow is inverted by 10 km.

The thickness of the sediments in the rift basin correlates with the size of the negative gravity anomaly (Figure 8). For example, model 13 has a 5 km thick sedimentary basin and a gravity anomaly of -35.5 mGal, whereas model 18 has a 15 km thick sedimentary basin with a gravity anomaly of -94.5 mGal. With inversion and removal of some sedimentary rock, the gravity anomaly is less negative. For

example, model 20 has a 15 km thick sedimentary basin with a tectonic inversion of 10 km, yielding a gravity anomaly of -50 mGal compared to -94 mGal before inversion.

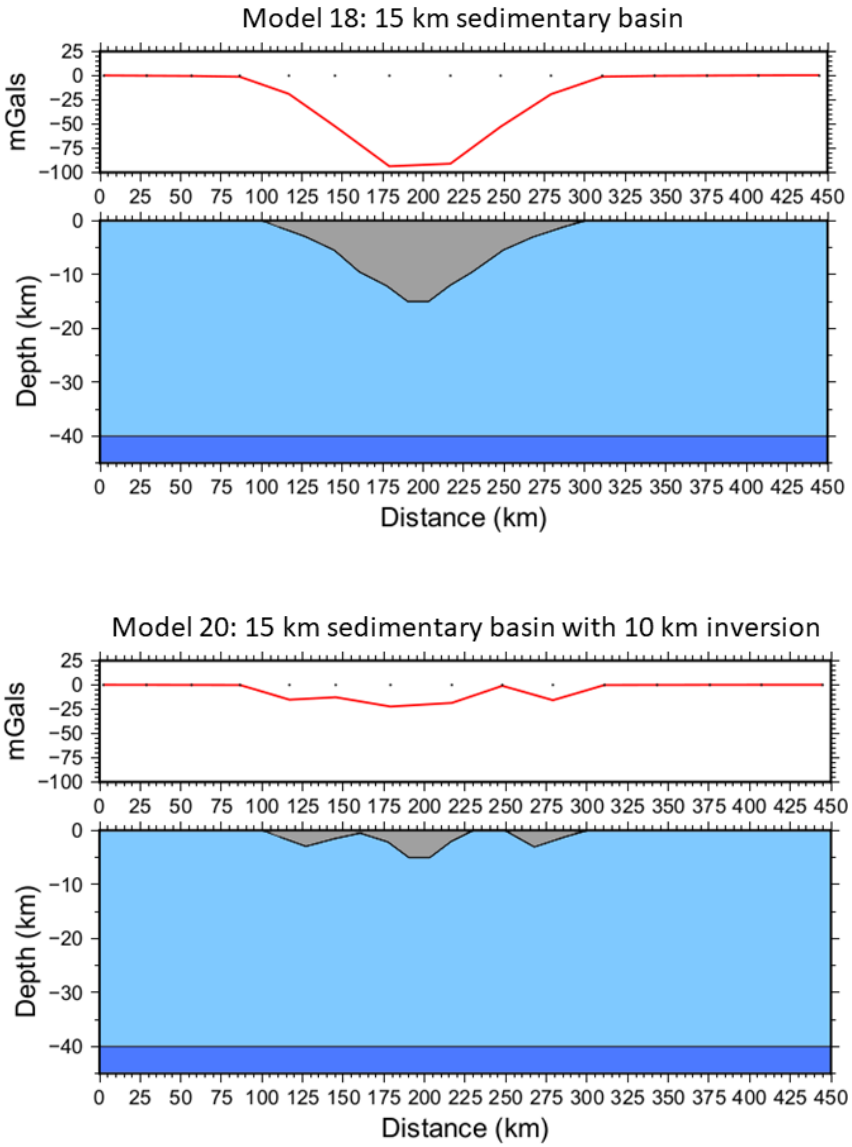

Figure 8. Schematic gravity models 18 (top) and 20 (bottom). Black dots are gravity at 0 mGal, red line is calculated gravity, light blue layer is crust, dark blue layer is mantle, and gray layer is sedimentary basin. Model 18 (top) illustrates a -94 mGal gravity anomaly created by a 15 km deep sedimentary basin, and model 20 (bottom) demonstrates the decrease in gravity anomaly to -22 mGal when the sedimentary basin is inverted by 10 km.

Thus, these 20 basic models for the gravity analysis answer the first question in Section 1.4 and illustrate the effect of varying geologic structures at varying depths, with and without inversions. With this basic understanding of the relationship between geologic structures and gravity anomalies, I next examined the Reelfoot Rift and Southern Oklahoma Aulacogen.

4.2 **Reelfoot Rift Models**

The first Reelfoot Rift model I created was to reproduce the gravity data and cross-section from Figure 4 (Liu et al., 2017). The first run of this model had contradictory results—while I was able to replicate the cross-section, using the densities given by Liu et al. (2017) resulted in a maximum gravity anomaly that was significantly different than their published results (Figure 9). I performed a root-mean-square error (RMSE) analysis on each model built to check for its measure of fit. This model compared to the observed gravity data had an RMSE of 41.5 mGal.

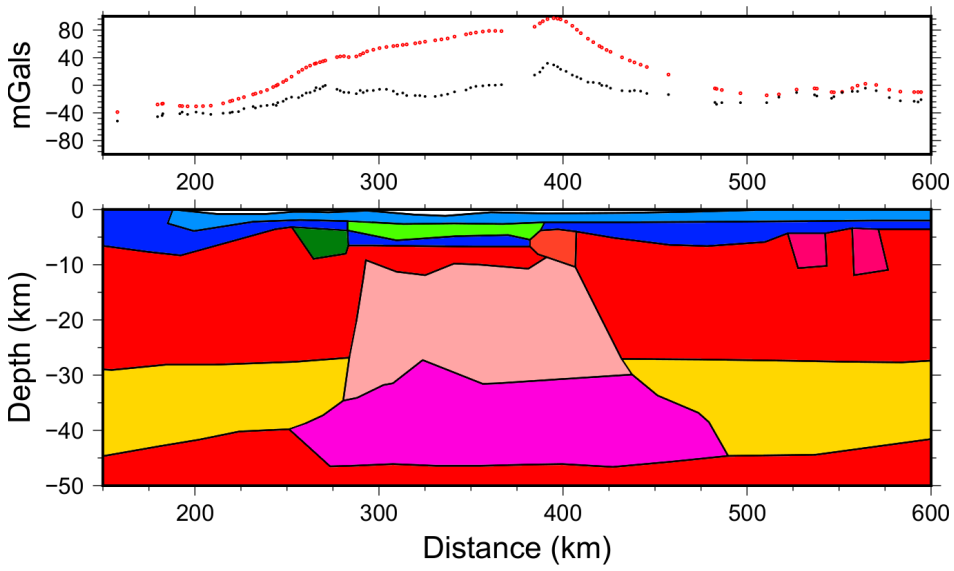

Figure 9. Reproduction of the Reelfoot Rift model from Liu et al. (2017). Black dots are the observed gravity anomalies, and red dots are the model's calculations. Colored layers for Reelfoot Rift are the same as Figure 4.

For the second run of the model, I changed the density of the rift pillow (the high-density lower crust layer) to 3.02 g/cm³ from the 3.15 g/ cm³ used by Liu et al. (2017) (Figure 4). This replicated their results with an RMSE of 8.3 mGal (Figure 10). With an understanding that modeled densities of subsurface structures based on seismic velocity data can vary up to 0.1 g/cm³ or more at depth (Keller, correspondence), that previous studies of the Reelfoot Rift gave the rift pillow densities of 3.0 g/cm³ and 3.1 g/cm³ (Mooney, et al., 1983; Stuart et al., 1997), and that Liu et al. (2017) adjusted their densities by up to 15% in order to match observed gravity data, I deemed this an adequate fit for the data.

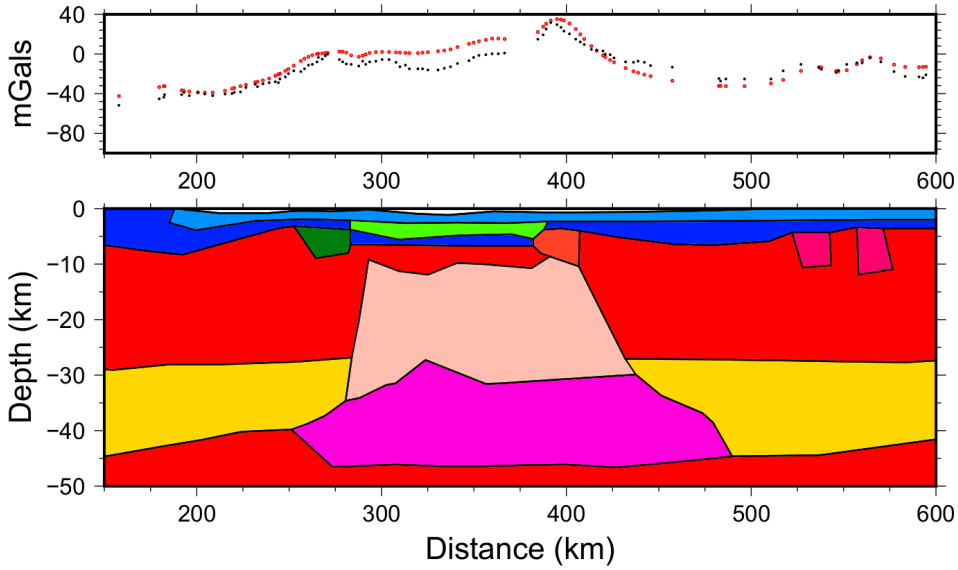

Figure 10. Reproduction of the Reelfoot Rift model with a lower density for the rift pillow compared to Figure 9. Adapted from Liu et al. (2017). Black dots are the observed gravity anomalies, and red dots are the model's calculations. Colored layers for Reelfoot Rift are the same as Figure 4.

In the final model for the Reelfoot Rift region, the rift was inverted 10.5 km (Figure 11). As the Reelfoot Rift is already deemed to be inverted 1.5 km (Dart and Swolfs, 1998; Csontos et al., 2008), this gave a total inversion or uplift of 12 km. This amount is the same as the widely accepted uplift amount

for the Southern Oklahoma Aulacogen (Ham and Wilson, 1967; Perry, 1989; Robbins and Keller, 1992). This model creates a distinct Bouguer gravity high over the Reelfoot Rift with a maximum gravity anomaly of 171 mGal. Unsurprisingly, the goodness-of-fit for this model compared to the observed gravity data was quite low, with an RMSE of 66.8 mGal. In Section 5, I will directly compare the gravity anomalies for Figure 11 of the Reelfoot Rift with the observed gravity anomalies for the Southern Oklahoma Aulacogen in Figure 6.

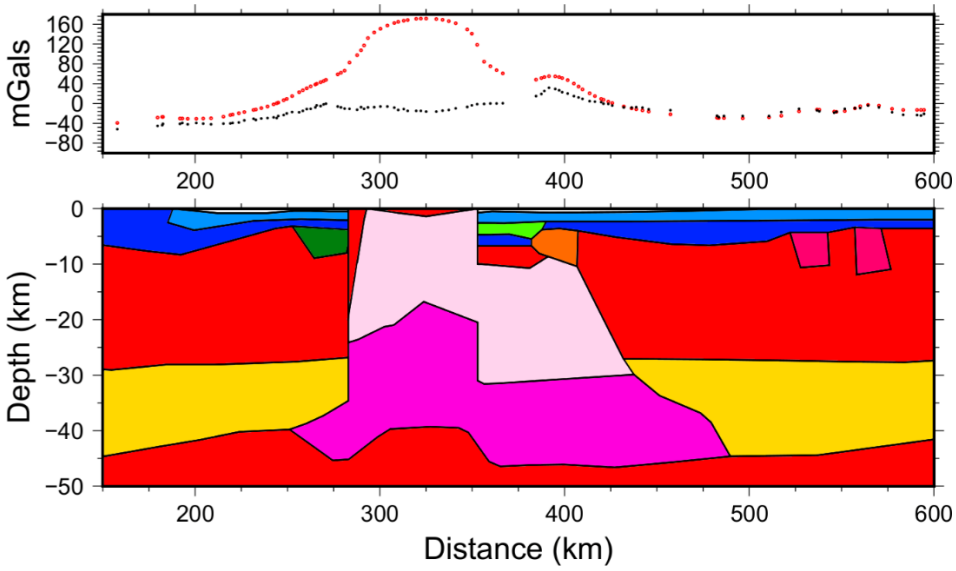

Figure 11. Model of Reelfoot Rift with an inversion of 10.5 km. Adapted from Liu et al. (2017). Black dots are the observed gravity anomalies, and red dots are the model's calculations. Colored layers for Reelfoot Rift are the same as Figure 4.

4.3 **Southern Oklahoma Aulacogen Models**

Similar to the study for the Reelfoot Rift, I first reproduced the cross-section and gravity anomalies for the Southern Oklahoma Aulacogen (Keller and Stephenson, 2007) (Figure 12). The

goodness-of-fit based on a RMSE analysis between the observed and calculated gravity anomalies is 6.5 mGal, verifying the reproduction's overall robustness.

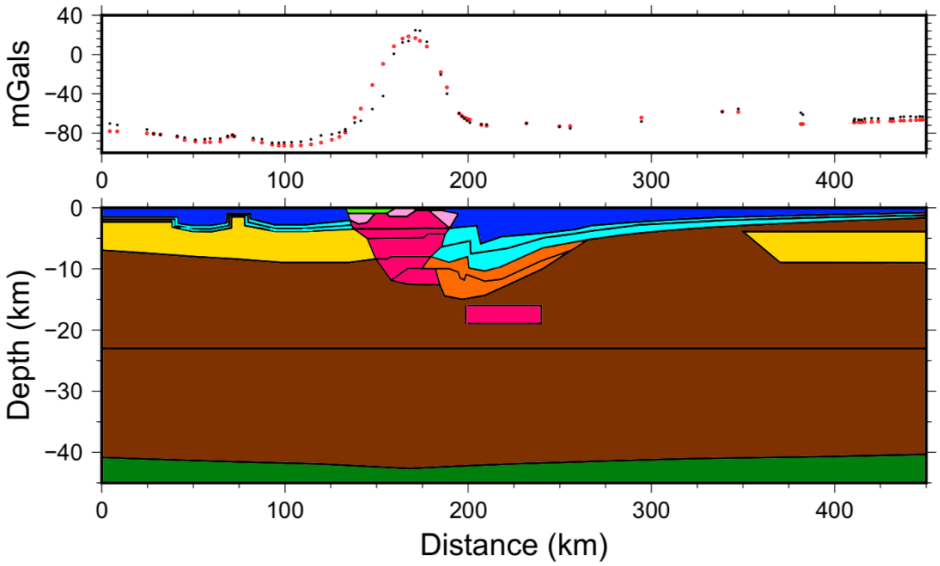

Figure 12. Reproduction of the Southern Oklahoma Aulacogen model from Keller and Stephenson (2007). Black dots are the observed gravity anomalies, and red dots are the model's calculations. Colored layers for Southern Oklahoma Aulacogen are the same as Figure 6.

The second question for this study was whether a rift pillow at the base of the crust below the Southern Oklahoma Aulacogen could be consistent with the gravity data. As mentioned earlier, an underplated, high-density lower crust layer is a signature of many continental rift zones (Mooney et al., 1983; White and McKenzie, 1989) due to the residuum from mafic magma upwelling from the mantle during rifting (Zoback and Richardson, 1996; Thybo and Artemieva, 2013). A rift pillow beneath the Southern Oklahoma Aulacogen has not been identified in the literature. While this region has been studied extensively due to the wealth of economic resources associated with the Anadarko Basin, much of these studies are proprietary, and published studies didn't have adequate resolution at a depth

expected for a rift pillow. To examine the gravity effect, I ran this model with 5 km and 10 km rift pillows (Figure 13), which produced RMSEs of 7.6 mGal and 9.9 mGal, respectively. To make either rift pillow fit the gravity signature, I used a density of 3.05 g/cm³ compared to the 3.02 g/cm³ density I used for the pillow beneath the Reelfoot Rift (Figure 10).

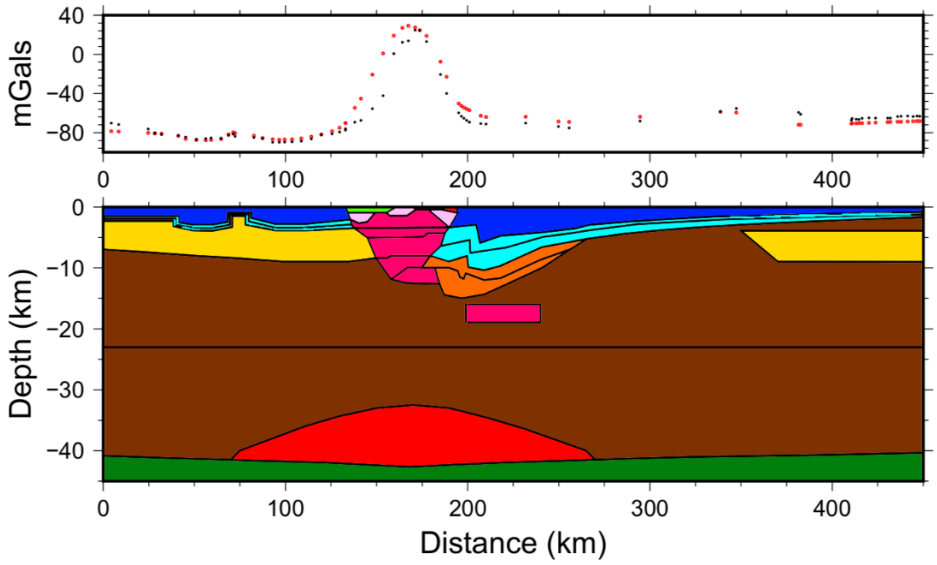

Figure 13. Model of the Southern Oklahoma Aulacogen with a 10-km thick rift pillow. Adapted from Keller and Stephenson (2007). Black dots are the observed gravity anomalies, and red dots are the model's calculations. Colored layers for Southern Oklahoma Aulacogen are the same as Figure 6.

For the next model, I uplifted this pillow 12 km to make it equivalent to the uplift of the rest of the structures of the Southern Oklahoma Aulacogen (Figure 14). To make the model of the inverted rift pillow align with the gravity profile, some of the underlying densities were changed (Table II). Even with these adjustments, the fit here was not quite as close with an RMSE of 10.4 mGal, but it was closer than that of the 12-km-inverted 5-km-thick rift pillow model (RMSE of 14.6 mGal). For the study, I used the 10

km rift pillow model due to its: 1) closer size to that of the Reelfoot Rift rift pillow and 2) better "fit" when uplifted.

Layer	Keller & Stephenson (2007) Densities (g/cm³)	Modeled Density (g/cm³)
Rift Pillow	3.15	3.01
Gabbro 4	3.05	2.95
Gabbro 5	3.10	3.00
Rift Fill	2.63	2.60
Carlton Rhyolite	2.72	2.70
Lower Paleozoic (lower)	2.75	2.70
Lower Paleozoic (upper)	2.63	2.60

Table II. Density adjustments made to Southern Oklahoma Aulacogen with 10 km rift pillow model.

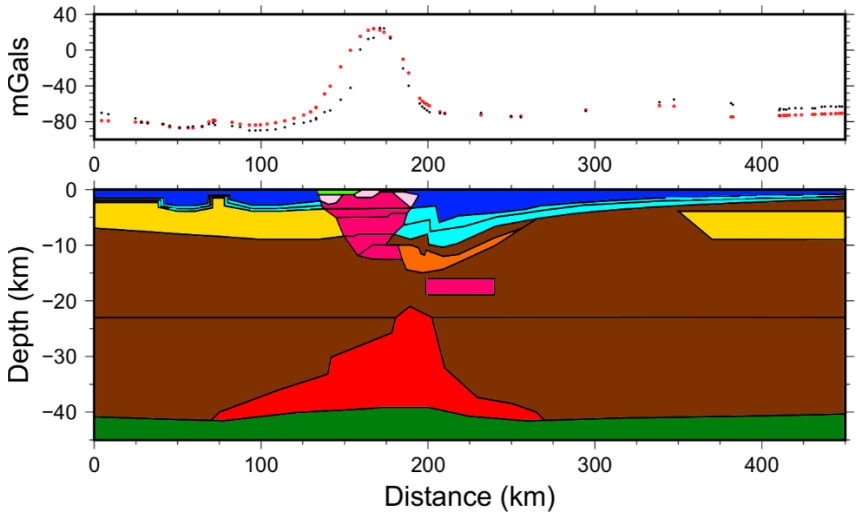

Figure 14. Model of the Southern Oklahoma Aulacogen with a 10-km thick rift pillow that has been inverted 12 km. Adapted from Keller and Stephenson (2007). Black dots are the observed gravity anomalies, and red dots are the model's calculations. Colored layers for Southern Oklahoma Aulacogen are the same as Figure 6.

Finally, for the last model, (Figure 15) I uninverted or subsided the center of the Southern Oklahoma Aulacogen 10.5 km so that its total uplift amount would be 1.5 km and would thus be comparable to the Reelfoot Rift as discussed in Section 4.5.

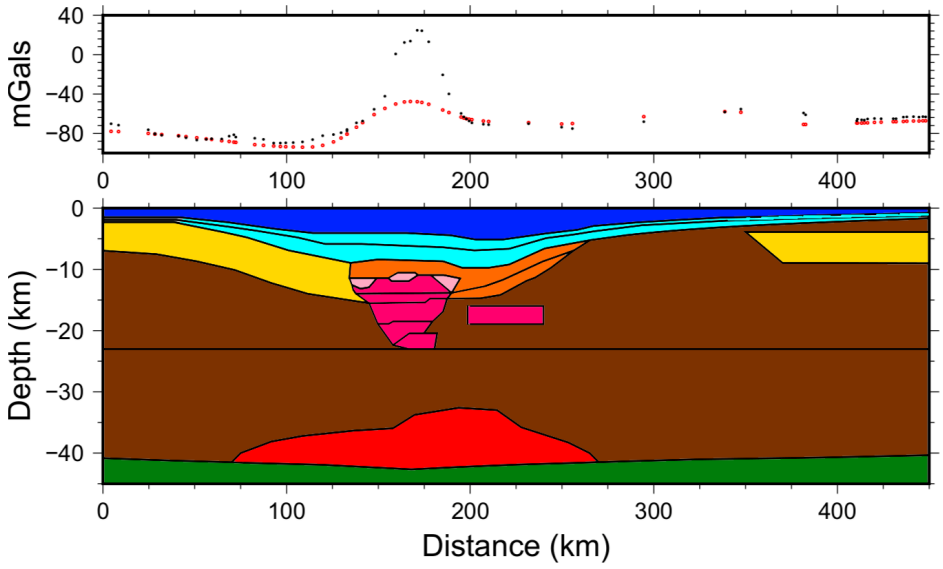

Figure 15. Model of the Southern Oklahoma Aulacogen with a 10-km thick rift pillow that has been subsided 10.5 km. Adapted from Keller and Stephenson (2007). Black dots are the observed gravity anomalies, and red dots are the model's calculations. Colored layers for Southern Oklahoma Aulacogen are the same as Figure 6.

4.4 **Inverted Reelfoot Rift Compared to the Southern Oklahoma Aulacogen**

The primary difference between the Reelfoot Rift and Southern Oklahoma Aulacogen is the latter's extreme inversion. To compare these rifts, I isolated and altered characteristics of one of the rifts to match the other. As discussed earlier, the Reelfoot Rift has approximately 1.5 km of inversion (Dart and Swolfs, 1998; Csontos et al., 2008), whereas the Southern Oklahoma Aulacogen has 12 km of

inversion (Ham and Wilson, 1967; Perry, 1989; Robbins and Keller, 1992). To compare the rifts, I uplifted the Reelfoot Rift an additional 10.5 km to make the amount of rift inversion roughly equivalent. Both rifts then have a distinctive Bouguer gravity high (Figure 16). The maximum gravity anomalies, however, differ significantly, with the Reelfoot Rift having a maximum gravity anomaly of 171 mGal and the Southern Oklahoma Aulacogen having a maximum gravity anomaly of 25 mGal. Because of the different baselines of the gravity anomalies of the Southern Oklahoma Aulacogen and Reelfoot Rift, it was necessary to make adjustments prior to running the statistical analysis. For the RMSE I considered 270 km across the profiles, adjusted the baseline of the inverted Reelfoot Rift -65 mGal, and matched up the gravity anomalies by their relative x-value before running the analysis. With an absolute difference in gravity anomalies at 146 mGal, the goodness-of-fit for the data across these rifts was poor at 34.8 mGal.

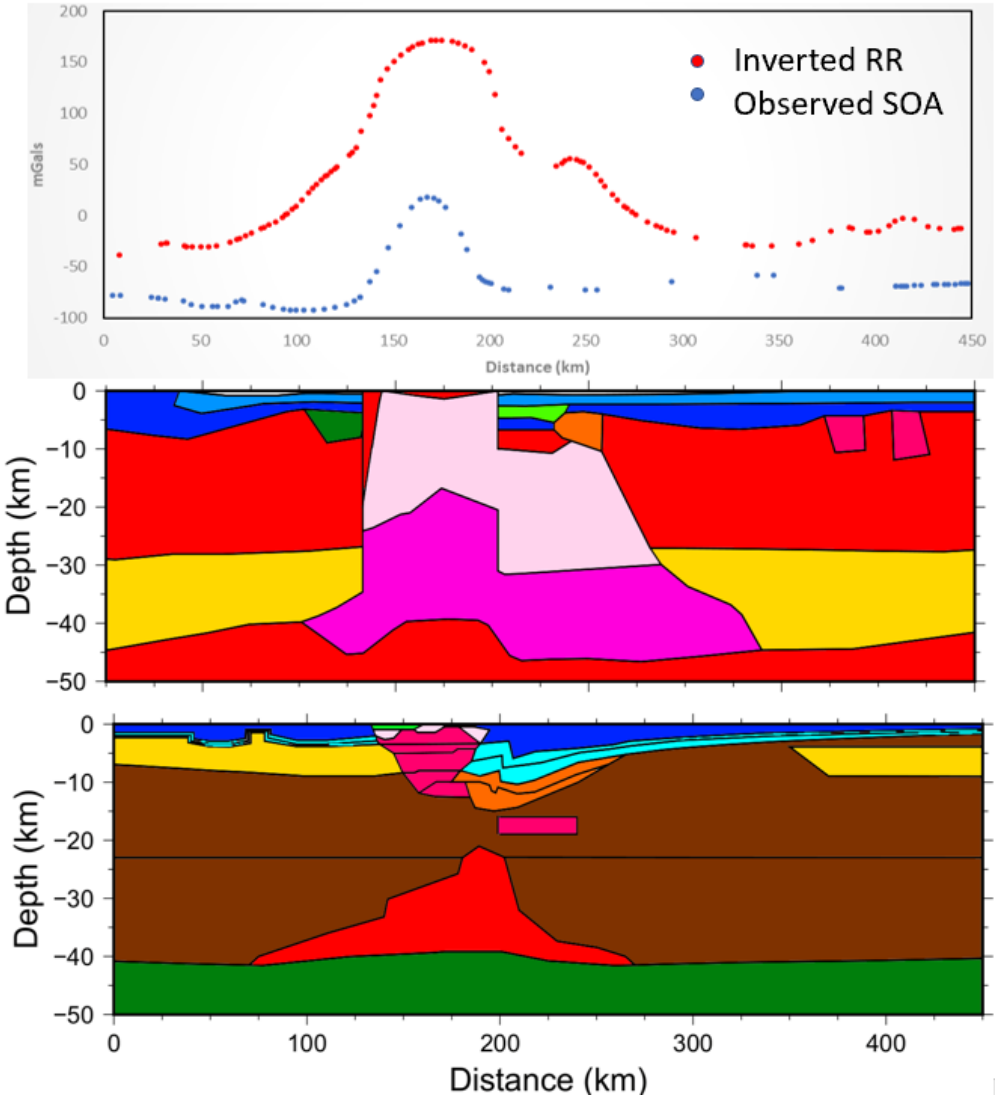

Figure 16. Side-by-side comparison of models of the Reelfoot Rift inverted 10.5 km (middle) and the observed Southern Oklahoma Aulacogen (bottom). Adapted from Liu et al. (2017) and Keller and Stephenson (2007). Blue dots are the observed gravity anomalies for SOA, and red dots are the model's calculations from Figure 11 (top). Colored layers for the Reelfoot Rift are the same as Figure 4, and those for the Southern Oklahoma Aulacogen are the same as Figure 6.

4.5 Uninverted Southern Oklahoma Aulacogen Compared to the Reelfoot Rift

To compare the relatively uninverted state of the rifts, I "subsided" the Southern Oklahoma Aulacogen by 10.5 km to make it correspond to the Reelfoot Rift's 1.5 km of inversion (Dart and Swolfs,

1998; Csontos et al., 2008) (Figure 17). The “uninverted” Southern Oklahoma Aulacogen still has a positive gravity anomaly compared to the negative gravity anomaly across the Reelfoot Rift, but the maximum value decreased from 25 mGal to -47 mGal, a 72 mGal swing in the opposite direction. However, even though there is a distinctive visual difference between the gravity anomalies, the RMSE suggested a better goodness-of-fit for the data across these rifts compared to the results in Section 5.1 at 23.1 mGal. Similar adjustments as discussed in the previous section were made to run the statistical analysis. The RMSE used datapoints from 270 km across the profiles, the baseline of the uninverted Southern Oklahoma Aulacogen was adjusted +65 mGal, and the gravity anomalies were matched by their relative x-value before running the analysis.

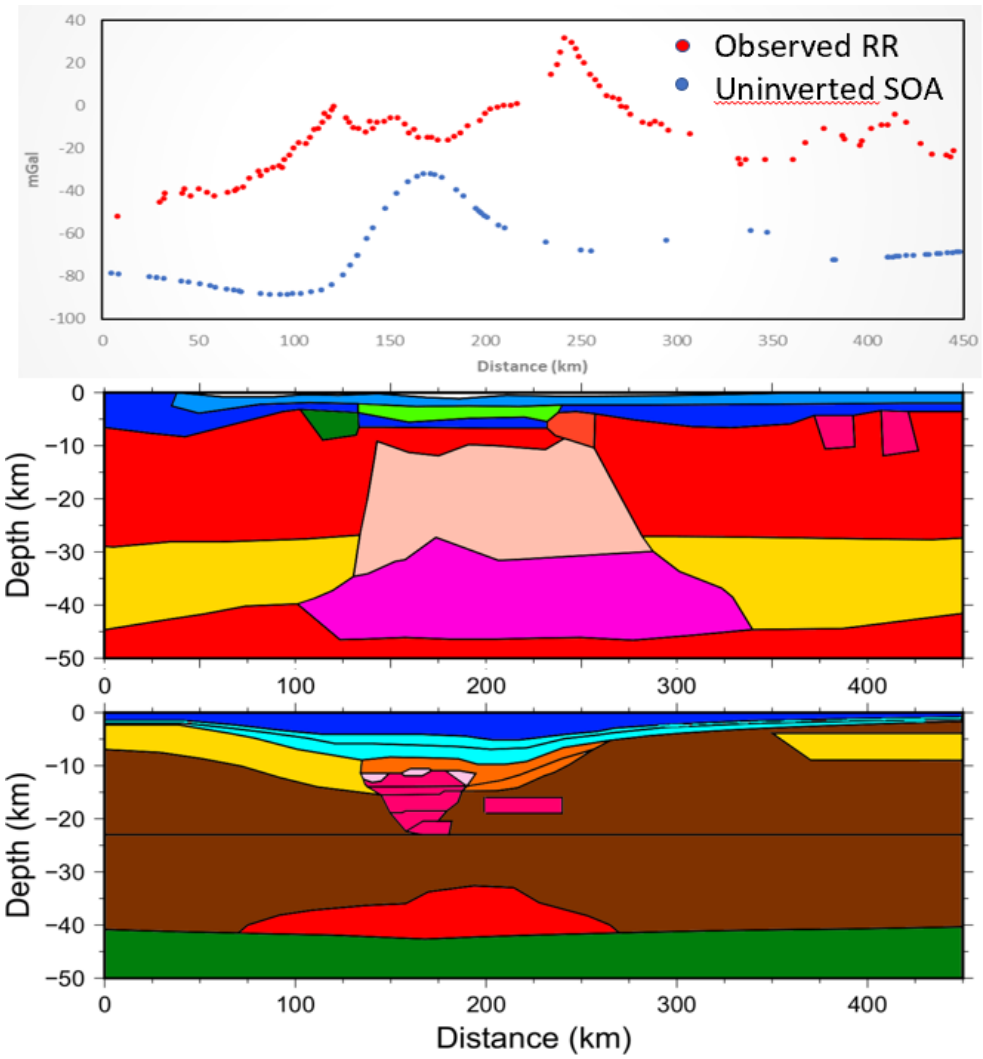

Figure 17. Side-by-side comparison of models of the Reelfoot Rift (middle) and the Southern Oklahoma Aulacogen (bottom) uninverted 10.5 km with a 10-km thick rift pillow. Adapted from Liu et al. (2017) and Keller and Stephenson (2007). Blue dots are the model's calculations for the SOA (Figure 15), and red dots are the observed Reelfoot Rift gravity anomalies (top). Colored layers for Reelfoot Rift are the same as Figure 4, and those for the Southern Oklahoma Aulacogen are the same as Figure 6.

5. DISCUSSION

The schematic models (Section 4.1) illustrated the effect of rift pillows, sedimentary basins, and inversion on gravity anomalies, thus answering the first question. Rift pillows create positive gravity anomalies, sedimentary basins create negative gravity anomalies. The thickness of each increases the effect, and rift pillow proximity to the surface increases the strength of the gravity anomaly.

For the second question, the Southern Oklahoma Aulacogen models (Section 4.3) showed that 5-10 km thick rift pillows could fit the observed gravity anomaly of the Southern Oklahoma Aulacogen. Even when those rift pillows are inverted, and thus brought closer to the surface, these pillows can “fit”.

This study could not definitively answer the third question as to whether the Reelfoot Rift and Southern Oklahoma Aulacogen can be considered as analogs of one another at different stages in rift evolution. Although I was able to isolate the effects of the inversion and manipulate the conditions of the rifts so they could be compared to one another, the gravity profiles were not that similar. Inverting the Reelfoot Rift 10.5 km did produce a large positive gravity anomaly, but it was considerably greater than the gravity anomaly for the Southern Oklahoma Aulacogen. Additionally, subsiding the Southern Oklahoma Aulacogen 10.5 km did reduce its positive gravity anomaly, but it did not produce a negative gravity anomaly that would match that of the Reelfoot Rift.

This study partially answered the fourth question as to why the gravity profiles are so different between the rifts. Some lithology differences between the two rifts may account for some of the mismatch. At the Reelfoot Rift, there are mafic bodies relatively close to the surface on either side of the rift that have an influence on the gravity anomaly. It has been suggested that the Bermuda hotspot may have crossed the Reelfoot Rift, altering the lithology and associated densities (Pollitz and Mooney, 2014). In addition, the Midcontinent Rift with its thick “flood” basalts is proposed to extend into the region of the Southern Oklahoma Aulacogen (Robbins and Keller, 1992) and so the pre-rift geology would be different than the Reelfoot Rift.

This study builds upon the extensive body of research into the Reelfoot Rift and Southern Oklahoma Aulacogen regions by comparing their differences and similarities. This study showed that a rift pillow could exist below the Southern Oklahoma Aulacogen. While these models did not provide definitive results to conclude that these rifts could be considered analogs at different stages of evolution, I do think they are similar enough to warrant additional inquiry. In the future, additional

models could be made to further constrain the differences between the rifts. For example, could the relatively shallow mafic intrusions in the Reelfoot Rift be replaced by pre-intruded, lower density material? How would this affect the model? Furthermore, these rifts could be modeled with different amounts of inversion. While most studies give 12 km as the inversion on the rift, there are a couple of papers that give an inversion of 15 km (Keller and Baldridge, 1995; Keller and Stephenson, 2007). Additionally, whether the Reelfoot Rift did have an inversion of 1.5 km is not universally accepted.

While this study modeled the uplifted Reelfoot Rift in a way that brought the entire mafic upper crust and rift pillow closer to the surface, realistic changes in shape and size of the uplifted region were not included here. One issue to explore is the effect on the gravity signature if the reverse faulting does not extend into the lower crust and rift pillow. One possibility is that the inversion-inducing compression would squeeze the pillow, pushing some of the pillow material down towards the mantle, much like the crustal root underneath a mountain. If the Reelfoot Rift were modeled with an inversion in this way, the gravity profile might be much closer to that of the Southern Oklahoma Aulacogen, rather than the significantly greater magnitude currently modeled (Figure 16). Similarly, the range in values for the dips of the faults in the subsidence for the Southern Oklahoma Aulacogen and for the uplift for the faults of the Reelfoot Rift could be explored.

6. REFERENCES

Baldridge, W.S., Keller, G.R., and Braile, L.W., 1995, Continental rifting: A final perspective *in* Olsen, K.H., ed., Continental rifts: Evolution, structure, tectonics: Publication No. 264 of the International Lithosphere Program Developments in Geotectonics 25, Elsevier, p. 453-459.

Bott, M.H.P., and Hinze, W.J., 1995, Potential field methods, *in* Olsen, K.H., ed., Continental rifts: Evolution, structure, tectonics: Publication No. 264 of the International Lithosphere Program Developments in Geotectonics 25, Elsevier, p. 93-98.

Braile, L.W., Hinze, W.J., Keller, G.R., Lidiak, E.G., and Sexton, J.L., 1986, Tectonic development of the New Madrid Rift Complex, Mississippi Embayment, North America: Tectonophysics, v. 131, p. 1-21.

Brewer, J.A., Good, R., Oliver, J.E., Brown, L.D., Kaufman, S., 1983, COCORP profiling across the Southern Oklahoma Aulacogen: Overthrusting of the Wichita Mountains and compression within the Anadarko Basin: Geology, v. 11, p. 109-114.

Brueseke, M.E., Hobbs, J.M., Bulen, C.L., Mertzman, S.A., Puckett, R.E., Walker, J.D., and Feldman, J., 2016, Cambrian intermediate-mafic magmatism along the Laurentian margin: Evidence for flood basalt volcanism from well cuttings in the Southern Oklahoma Aulacogen (U.S.A.): Lithos, v. 260, p. 164-177.

Brun, J.P., and Choukroune, P., 1983, Normal faulting, block tilting and decollement in a stretched crust: Tectonics, v. 2, p. 345-356.

Buck, W.R., 2007, Dynamic processes in extensional and compressional settings: The dynamics of continental breakup and extension *in* Treatise on Geophysics: Elsevier, v. 6. p. 335-376. doi: 10.1016/B978-044452748-6.00110-3.

Burke, K., 1977, Aulacogens and continental breakup: Annual Review of Earth and Planetary Sciences, v. 5, p. 371-396.

Burke, K., and Dewey, J.F., 1973, Plume-generated triple junctions: Key indicators in applying plate tectonics to old rocks: The Journal of Geology, v. 81, n. 4, p. 406-433.

Cady, J.W., 1980, Calculation of gravity and magnetic anomalies of finite-length right polygonal prisms: Geophysics, v. 45, n. 10, p. 1507-1512.

Catchings, R.D., 1999, Regional Vp, Vs, Vp/Vs, and Poisson's ratios across earthquake source zones from Memphis, Tennessee, to St. Louis, Missouri: Bulletin of the Seismological Society of America, v. 89, n. 6, p. 1591-1605.

Chang, W.F., McMechan, G.A., and Keller, G.R., 1989, Wave field processing of data from a large-aperture seismic experiment in Southwestern Oklahoma: Journal of Geophysical Research, v. 94, n. B2, p. 1803-1816.

Chen, C., Zhao, D., and Wu, S., 2014, Crust and upper mantle structure of the New Madrid Seismic Zone: Insight into intraplate earthquakes: Physics of the Earth and Planetary Interiors, v. 230, p. 1-14.

Csontos, R., Van Arsdale, R., Cox, R., and Waldron, B., 2008, Reelfoot rift and its impact on Quaternary deformation in the central Mississippi River valley: Geosphere, v. 4, n. 1, p. 145-158.

Dalziel, I.W., 1997, Neoproterozoic-Paleozoic geography and tectonics: Review, hypothesis, environmental speculation: Geological Society of America Bulletin, v. 109, n. 1, p. 16-42.

Dart, R.L., and Swolfs, H.S., 1998, Contour mapping of relic structures in the Precambrian basement of the Reelfoot Rift, North American midcontinent: Tectonics, v. 17, n. 2, p. 235-249.

Ekström, G., 2017, Short-period surface-wave phase velocities across the conterminous United States: Physics of the Earth and Planetary Interiors, v. 270, p. 168-175.

Erkan, K., 2015, Geophysical investigations on gravity gradiometry and magnetic data over the Wichita Uplift Region, Southwestern Oklahoma: Geodetic Science, n. 509, p. 1-22.

Ervin, C.P., and McGinnis, L.D., 1975, Reelfoot Rift: Reactivated precursor to the Mississippi Embayment: Geological Society of America Bulletin, v. 86, p. 1287-1295.

Evanzia, D., Pulliam, J., Ainsworth, R., Gurrola, H., and Pratt, K., 2014, Seismic Vp & Vs tomography of Texas & Oklahoma with a focus on the Gulf Coast margin: Earth and Planetary Science Letters, v. 402, p. 148-156.

Gallegos, A., Ranasinghe, N., Ni, J., and Sandvol, E., 2014, Lg attenuation in the central and eastern United States as revealed by the EarthScope Transportable Array: Earth and Planetary Science Letters, v. 402, p. 187-196.

Green, A.G., Cannon, W.F., Milkereit, B., Hutchinson, D.R., Davidson, A., Behrendt, J.C., Spencer, C., Lee, M.W., Morel-á-LáHuissier, P., and Agena, W.F., 1989, A “GLIMPCE” of the deep crust beneath the Great Lakes *in* Mereu, R.F., Mueller, S., and Fountain, D.M., eds., Properties and processes of Earth's lower crust: Geophysical Monograph Series 51, American Geophysical Union, pp. 65–80.

Ham, W.E., and Wilson, J.L., 1967, Paleozoic epeirogeny and orogeny in the central United States: American Journal of Science, v. 265, p. 332-407.

Hanson, R.E., Puckett, R.E., Keller, G.R., Brueseke, M.E., Bulen, C.L., Mertzman, S.A., Finegan, S.A., and McCleery, D.A., 2013, Intraplate magmatism related to opening of the southern Iapetus Ocean, Cambrian Wichita igneous province in the Southern Oklahoma rift zone: Lithos, v. 174, p. 57–70.

Hanson, R.E., and Eschberger, A.M., 2014, An Overview of the Carlton Rhyolite Group: Cambrian A-type felsic volcanism in the Southern Oklahoma Aulacogen: Oklahoma Geological Survey Guidebook 38, p. 123-142.

Hildenbrand, T.G., 1985, Rift structure of the northern Mississippi from the analysis of gravity and magnetic data: Journal of Geophysical Research, v. 90, p. 12607-12622.

Howe, J.R., 1985, Tectonics, sedimentation, and hydrocarbon potential of the Reelfoot aulacogen: Master's thesis, University of Oklahoma, Norman, 109 p.

Howe, J.R., and Thompson, T.L., 1984, Tectonics, sedimentation, and hydrocarbon potential of the Reelfoot Rift: Oil and Gas Journal, v. 82, p. 179-190.

Huismans, R.S., and Beaumont, C., 2009, Structural style of inversion of rifts and passive margins: feedback between mountain building and surface processes: Trabajos de Geología, Universidad de Oviedo, v. 29, p. 349-354.

Ingersoll, R.V., 2012, Tectonics of sedimentary basins, with revised nomenclature *in* Busby, C., and Azor, A., eds., Tectonics of Sedimentary Basins: Recent Advances, p. 3-30.

Kane, M.F., Hildenbrand, T.G., and Hendricks, J.D., 1981, Model for the tectonic evolution of the Mississippi embayment and its contemporary seismicity: Geology, v. 9, p. 563-568.

Keller, G.R., and Baldridge, W.S., 1995, The Southern Oklahoma Aulacogen, *in* Olsen, K.H., ed., Continental rifts: Evolution, structure, tectonics: Publication No. 264 of the International Lithosphere Program Developments in Geotectonics 25, Elsevier, p. 427-436.

Keller, G.R., and Stephenson, R.A., 2007, The Southern Oklahoma and Dniepr-Donets aulacogens: A comparative analysis, *in* Hatcher, R.D., Jr., Carlson, M.P., McBride, J.H., and Martínez Catalán, J.R., eds., 4-D Framework of continental crust: Geological Society of America Memoir 200, p. 1-17.

Kolata, D.R., and Nelson, W.J., 1991, Tectonic history of the Illinois basin, *in* Leighton, M.W., et al., eds., Interior Cratonic Basins: AAPG Memoirs, v. 51, p. 263-286.

Liu, L., Gao, S.S., Liu, K.H., and Mickus, K., 2017, Receiver function and gravity constraints on crustal structure and vertical movements of the Upper Mississippi Embayment and Ozark Uplift: Journal of Geophysical Research: Solid Earth, v. 122, p. 4572-4583.

Lowrie, W., 2004, Fundamentals of Geophysics: New York, Cambridge University Press, 354 p.

McGlannan, A.J., and Gilbert, H., 2016, Crustal signatures of the tectonic development of the North American midcontinent: Earth and Planetary Science Letters, v. 433, p. 339-349.

Mooney, W.D., Andrews, M.C., Ginzburg, A., Peters, D.A., and Hamilton, R.M., 1983, Crustal structure of the northern Mississippi embayment and a comparison with other continental rift zones: Tectonophysics, v. 94, p. 327-348.

Nelson, K.D., and Zhang, J., 1991, A COCORP deep reflection profile across the buried Reelfoot Rift, south-central United States: Tectonophysics, v. 197, p. 271-293.

Northcutt, R.A., and Campbell, J.A., 1998, Geologic Provinces of Oklahoma *in* Hogan, J.P., and Gilbert, M.C., eds., Basement Tectonics 12: Proceedings of the International Conferences on Basement Tectonics, v. 6., p. 29-37.

Olsen, K.H., and Morgan, P., 1995, Introduction: Progress in understanding continental rifts, *in* Olsen, K.H., ed., Continental rifts: Evolution, structure, tectonics: Publication No. 264 of the International Lithosphere Program Developments in Geotectonics 25, Elsevier, p. 3-26.

Perry, W.J., 1989, Tectonic evolution of the Anadarko basin region, Oklahoma: United States Geological Survey Bulletin 1866-A, 19 p.

Pollitz, F.F., and Mooney, W.D., 2014, Seismic structure of the Central US crust and shallow upper mantle, Uniqueness of the Reelfoot Rift: Earth and Planetary Science Letters, v. 402, p. 157-166.

Pollitz, F.F., and Mooney, W.D., 2016, Seismic velocity structure of the crust and shallow mantle of the Central and Eastern United States by seismic surface wave imaging: Geophysical Research Letters, v. 43, p. 118-126.

Robbins, S.L., and Keller, G.R., 1992, Complete Bouguer and isostatic residual gravity maps of the Anadarko Basin, Wichita Mountains, and surrounding areas, Oklahoma, Kansas, Texas, and Colorado, *in* U.S. Geological Survey Bulletin 1866-G, p. 1-11.

Rohatgi, A., 2015, WebPlotDigitizer: Austin, Texas: http://arohatgi.info/WebPlotDigitizer.

Salayandia, L., Keller, R., Aldouri, R., and Whitelaw, J., 2004, Talwani gravity modeling program: University of Texas at El Paso, https://research.utep.edu/default.aspx?tabid=45290.

Schnabel, M., Franke, D., Engels, M., Hinz, K., Neben, S., Damm, V., Grassmann, S., Pelliza, H., and Dos Santos, P.R., 2008, The structure of the lower crust at the Argentine continental margin, South Atlantic at 44 S: Tectonophysics, v. 454, n. 1–4, p. 14–22.

Scotese, C.R., 2009, Late Proterozoic plate tectonics and palaeogeography: A tale of two supercontinents, Rodinia and Pannotia: Geological Society, London, Special Publications, v. 326, n. 1, p. 67-83.

Stein, C.A., Kley, J., Stein, S., Hindle, D., and Keller, G.R., 2015, North America's Midcontinent Rift: When rift met LIP: Geosphere, v. 11, n. 5, p. 1607-1616, doi:10.1130/GES01183.1.

Stein, S., Stein, C.A., Elling, R., Kley, J., Keller, G.R., Wysession, M., Rooney, T., Frederiksen, A., Moucha, R., 2018, Insights from North America's failed Midcontinent Rift into the evolution of continental rifts and passive continental margins: Tectonophysics, v. 744, p. 403-421.

Stuart, W.D., Hildenbrand, T.G., and Simpson, R.W., 1997, Stressing of the New Madrid Seismic Zone by a lower crust detachment fault: Journal of Geophysical Research, v. 102, n. B12, p. 27,623-27,633.

Swan, F.H., Wesling, J.R., Hanson, K.A., Kelson, K.I., and Perman, R.C., 1993, Draft Report: Investigation of the Quaternary structural and tectonic character of the Meers Fault (Southwestern Oklahoma): Geomatrix Consultants, Inc., San Francisco, CA, 104 pp. plus appendices.

Talwani, M., Worzel, J.L., and Landisman, M., 1959, Rapid gravity computations for two-dimensional

bodies with application to the Mendocino submarine fracture zone: Journal of Geophysical Research, v. 64, n. 1, p. 49-59.

Thomas, W.A., 1991, The Appalachian-Ouachita rifted margin of southeastern North America: Geological Society of America Bulletin, v. 103, p. 415-431.

Thybo, R., and Artemieva, I.M., 2013, Moho and magmatic underplating in continental lithosphere: Tectonophysics, v. 609, p. 605-619.

Van Schmus, W.R., Bickford, M.E., and Turek, A., 1996, Proterozoic geology of the east-central mid-continent basement, *in*, van der Pluijm B.A., and Catacosinos, P.A. eds., Basement and Basins of Eastern North America: Geological Society of America, Special Paper 308, p.7-32.

White, R., and McKenzie, D., 1989, Magmatism at rift zones: The generation of volcanic continental margins and flood basalts: Journal of Geophysical Research, v. 94, n. B6, p. 7685-7729.

Whitmeyer, S.J., and Karlstrom, K.E., 2007, Tectonic model for the Proterozoic growth of North America: Geosphere, v. 3, n. 4, p. 220-259.

Williams, G.D., Powell, C.M., and Cooper, A., 1989, Geometry and kinematics of inversion tectonics: Geological Society, London, Special Publications, v. 44, p. 3-15.

Zoback, M.L., and Richardson, R.M., 1996, Stress perturbation associated with the Amazonas and other ancient continental rifts: Journal of Geophysical Research, v. 101, n. B3, p. 5459-5475.

VITA

Kerri M. Gefeke

Education

M.S. Candidate in Earth and Environmental Sciences; University of Illinois at Chicago; Present
- Advisor: Dr. Carol Stein

B.S. in Geology; Northern Illinois University; August 2017
- Magna Cum Laude
- Advisor: Dr. Jim Walker

B.A. in History; Augustana College (now Augustana University); May 1999
- Phi Alpha Theta Honor Society
- Cum Laude
- Advisor: Dr. Michael Mullin

Employment History

Graduate Teaching Assistant (2017-2019)
University of Illinois at Chicago; Chicago, IL.
- Carol Stein (Hydrology and Hydrogeology, Spring 2019)
- Stefany Sit (Earth, Energy, and the Environment, Fall 2017 & Fall 2018)
- Andrew Dombard (Earth, Energy, and the Environment, Spring 2018)

Geology Intern (Summer 2018)
United States Geological Survey, Earthquake Science Center, Menlo Park, CA.
- Supervisors: Keith Knudsen; Walter Mooney

Undergraduate Research Assistant (2017)
Northern Illinois University; DeKalb, IL.
- Supervisor: Dr. Nicole LaDue

Publication

Brocher, T.M., **Gefeke, K.M.,** Boatwright, J., and Knudsen, K.L., 2018, Reported investments in earthquake mitigation top $73 to $80 billion in the San Francisco Bay Area, California, since the 1989 Loma Prieta earthquake: USGS Open File Report 2018-1168. DOI: 10.3133/ofr20181168.

Conference Proceedings

Hultz, A.R., **Gefeke, K.M.,** and Balch, E., 2018, Detecting hidden faults in urban areas: Case studies and methodologies. Poster Presentation, Geological Society of America Abstracts with Programs, v. 50, n. 6. DOI: 10.1130/abs/2018AM-323868.

Plotnick, R., Bellagamba, A., Chancellor, S., Cunje, A., Dodd, E., **Gefeke, K.,** Hsieh, S., Pasterski, M.J., Schassburger, A., Smith, A., and Tucker, A., 2018, Historical Extirpations in Chicago Area Wetlands and Water Bodies, Paper presented to U.S. Regional Association of the International Association for Landscape Ecology (US-IALE), Chicago, IL, April 08-12, 2018.

Awards and Honors

2018 Outstanding Teaching Assistant Award from the National Association of Geoscience Teachers